0026-895X/06/6903-921–931$20.00
MOLECULAR PHARMACOLOGY
Copyright © 2006 The American Society for Pharmacology and Experimental Therapeutics
*Mol Pharmacol* 69:921–931, 2006

Vol. 69, No. 3
19257/3089433
*Printed in U.S.A.*



# Evidence for a Multivalent Interaction of Symmetrical, *N*-Linked, Lidocaine Dimers with Voltage-Gated $Na^+$ Channels

J. A. M. Smith, S. M. Amagasu, J. Hembrador, S. Axt, R. Chang, T. Church, C. Gee, J. R. Jacobsen, T. Jenkins,[1] E. Kaufman, N. Mai, and R. G. Vickery

*Theravance Inc., South San Francisco, California*

Received September 23, 2005; accepted December 9, 2005

## ABSTRACT

The interaction of symmetrical lidocaine dimers with voltage-gated $Na^+$ channels (VGSCs) was examined using a FLIPR membrane potential assay and voltage-clamp. The dimers, in which the tertiary amines of the lidocaine moieties are linked by an alkylene chain (two to six methylene units), inhibited VGSC activator-evoked depolarization of cells heterologously-expressing rat (r) $Na_v1.2a$, human (h) $Na_v1.5$, and $rNa_v1.8$, with potencies 10- to 100-fold higher than lidocaine (compound **1**). The rank order of potency ($C_4$ (compound **4**) > $C_3$ (compound **3**) ≥ $C_2$ (compound **2**) = $C_5$ (compound **5**) = $C_6$ (compound **6**) ≫ compound **1**) was similar at each VGSC. Compound **4** exhibited strong use-dependent inhibition of $hNa_v1.5$ with $pIC_{50}$ values <4.5 and 6.0 for tonic and phasic block, respectively. Coincubation with local anesthetics but not tetrodotoxin attenuated compound **4**-mediated inhibition of $hNa_v1.5$. These data suggest that the compound **4** binding site(s) is identical, or allosterically coupled, to the local anesthetic receptor. The dissociation rate of the dimers from $hNa_v1.5$ was dependent upon the linker length, with a rank order of compound **1** > compound **5** = compound **6** > compound **2** ≫ compound **3**. The observation that both the potency and dissociation rate of the dimers was dependent upon linker length is consistent with a multivalent interaction at VGSCs. $hNa_v1.5$ VGSCs did not recover from inhibition by compound **4**. However, "chase" with free local anesthetic site inhibitors increased the rate of dissociation of compound **4**. Together, these data support the hypothesis that compound **4** simultaneously occupies two binding sites on VGSCs, both of which can be bound by known local anesthetic site inhibitors.

VGSCs are transmembrane protein complexes that increase $Na^+$ permeability in response to membrane depolarization. Mammalian VGSCs consist of a pore-forming or $\alpha$ subunit, which is sufficient for functional channel expression, associated with one or more auxiliary $\beta$ subunits. The $\alpha$ subunit consists of four homologous domains (D1–D4), each of which has six transmembrane $\alpha$ helices (S1–S6) (Catterall, 2000). The VGSC is thought to be organized as a pseudotetramer with the S6 segments lining the inner surface of the channel pore (Sato et al., 2001). At least nine genes encoding VGSC $\alpha$ subunits have been identified ($Na_V1.1$–$Na_V1.9$), which can be differentiated based on their tissue distribution profiles and biophysical and/or pharmacological properties (Goldin et al., 2000).

In the plasma membrane, VGSCs interconvert between multiple conformational states (e.g., closed/resting, open, inactivated) in response to changes in membrane potential (Hille, 2001). The affinity of local anesthetics, which confer their activity by inhibiting the conduction of $Na^+$ ions through VGSCs and, thereby, action potential initiation/propagation in excitable tissues, depends upon the conformational state of the channel (Ragsdale et al., 1991). Local anesthetics bind to nonresting (i.e., open/inactivated states) with higher affinity than to resting states (Hondeghem and Katzung, 1977; Bean et al., 1983). The higher affinity of local anesthetics for the nonresting states is manifested as use dependence.

Receptors, ion channels, and enzymes that possess multiple binding sites due to symmetry, pseudosymmetry, or the presence of unrelated auxiliary sites may be targeted pharmacologically with dimeric ligands. Such an approach seeks to tether two ligands with a linker that can orient the ligands to bind the target simultaneously (Kiessling et al., 2000; Wright and Usher, 2001). The simultaneous occupation of two distinct concavities on a protein by such a bivalent ligand can confer upon it enhanced affinity, duration of action, and/or subtype selectivity relative to its component monomeric ligand(s) (Mammen et al., 1998). The critical parameters that control these properties are linker length, linker

[1] Current affiliation: Pharmacofore, Inc., Palo Alto, CA.

Article, publication date, and citation information can be found at http://molpharm.aspetjournals.org.
doi:10.1124/mol.105.019257.

**ABBREVIATIONS:** VGSC, voltage-gated $Na^+$ channel; h, human; r, rat; FMP, fluorescent membrane potential; 5-HT, 5-hydroxytryptamine; FLIPR, fluorometric imaging plate reader; ANOVA, analysis of variance; 4030W92, 2,4-diamino-5-(2,3-dichlorophenyl)-6-fluoromethylpyrimidine.

geometry and/or composition, ligand identity, and ligand attachment points.

Bivalent ligand design has been used successfully for such G-protein-coupled receptors as β-adrenergic (Kizuka and Hanson, 1987), κ opioid (Portoghese et al., 1988), muscarinic acetylcholine (Christopoulos et al., 2001), 5-$HT_{1A/D}$ (LeBoulluec et al., 1995) and 5-$HT_{1B/1D}$ (Halazy et al., 1996) receptors. Similar studies have also been undertaken for voltage-gated calcium channels (Joslyn et al., 1988) and $SK_{Ca}$ (Galanakis et al., 1996), nicotinic (Rosini et al., 1999), and cyclic nucleotide-gated (Kramer and Karpen, 1998) ion channels.

To the best of our knowledge, this approach has not been applied previously to VGSCs, although a number of structural features of VGSCs are consistent with the application of multivalent ligand design. In addition to the putative tetrameric organization of their four homologous domains, VGSCs also have six distinct binding sites for small molecules and peptide toxins (Cestele and Catterall, 2000). Based on the results of site-directed mutagenesis studies, it has been proposed that the S6 segments contribute to a domain-interface binding site for local anesthetics, analogous to that for antagonist binding in L-type $Ca^{2+}$ channels (Hockerman et al., 1997). Thus, amino acid residues in D1–S6 (Nau et al., 1999; Yarov-Yarovoy et al., 2002), D3–S6 (Wang et al., 2000; Yarov-Yarovoy et al., 2001), and D4–S6 (Ragsdale et al., 1996) have been proposed to participate in local anesthetic binding. However, other groups (Bennett et al., 1995; Kuroda et al., 1996, 2000) have proposed that, in addition to the D4–S6 conserved local anesthetic receptor, lidocaine also interacts with the D3–D4 cytoplasmic linker, which forms part of the inactivation domain. Furthermore, the existence of two independent binding sites for local anesthetics or small molecule VGSC inhibitors has been postulated (Lee-Son et al., 1992; Mujtaba et al., 2001, 2002; Leuwer et al., 2004).

In the present study, we examined the interaction of a series of symmetrical, *N*-linked lidocaine dimers, in which the nitrogens of each lidocaine moiety are tethered by an unsubstituted alkylene chain (two to six methylene units) (Fig. 1), with tetrodotoxin-sensitive ($Na_v1.2a$), tetrodotoxin-resistant ($Na_v1.8$), and cardiac ($Na_v1.5$) VGSC subtypes. CHO-K1, 293-EBNA, and F-11 cells stably transfected with $rNa_v1.2a$ ($rNa_v1.2a$-CHO), $hNa_v1.5$ ($hNa_v1.5$–293-EBNA), and $rNa_v1.8$ ($rNa_v1.8$-F-11), respectively, were used for FLIPR-based assays of membrane potential and whole-cell, voltage-clamp recordings. To characterize the interaction of dimers with native tetrodotoxin-resistant VGSCs, primary cultures of rat dorsal root ganglia neurons were used.

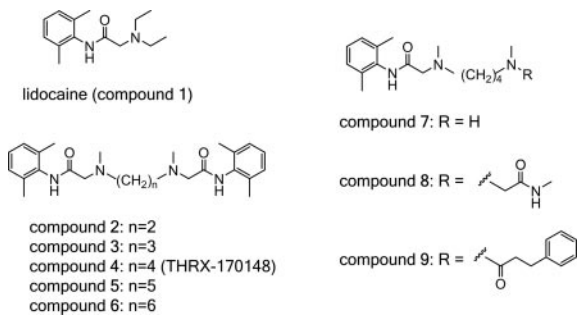


**Fig. 1.** Structures of lidocaine (compound **1**), symmetrical, *N*-linked lidocaine dimers, tethered by an unsubstituted alkylene linker ($n$ = 2 to 6 methylene units; compounds **2**-**6**) and three control molecules (compounds **7**, **8**, and **9**).

## Materials and Methods

**Cell Culture of $rNa_v1.2a$-CHO, $hNa_v1.5$–293-EBNA, and $rNa_v1.8$-F-11 Cells.** $rNa_v1.2a$-CHO cells were obtained under license from Dr. W. Catterall (University of Washington, Seattle, WA) and grown in RPMI 1640 medium containing 1 mM L-glutamine, supplemented with 5% heat-inactivated fetal bovine serum, 200 μg/ml G-418 (Geneticin), and 50 units/ml penicillin/50 μg/ml streptomycin. $hNa_v1.5$–293-EBNA cells were obtained under license from Dr. A. O. Grant (Duke University, Chapel Hill, NC) and grown in Dulbecco's modified Eagle's medium containing L-glutamine, supplemented with 5% heat inactivated fetal bovine serum, 50 μg/ml hygromycin, an additional 1 mM L-glutamine, and 50 units/ml penicillin/50 μg/ml streptomycin.

F-11 cells were obtained under license from Dr. M. Fishman (Harvard Medical School, Cambridge, MA). Untransfected F-11 and $rNa_v1.8$-F-11 cells were grown in Ham's F12 medium containing L-glutamine supplemented with 20% heat-inactivated fetal bovine serum, 1% hypoxanthine/aminopterin/thymidine (100 μM hypoxanthine, 0.4 μM aminopterin, and 16 μM thymidine), additional 1 mM L-glutamine and 50 units/ml penicillin/50 μg/ml streptomycin, in the absence and presence of 200 μg/ml geneticin (G-418), respectively. All cell lines were grown routinely as monolayers in an atmosphere of 95% $O_2$/5% $CO_2$ at 37°C.

For FLIPR studies, cells were seeded into black-walled, clear-bottomed, 96-well microtiter plates coated with poly-D-lysine (BD, Franklin Lakes, NJ). $rNa_v1.2a$-CHO and $hNa_v1.5$–293-EBNA cells were seeded at optimized concentrations of $50 \times 10^3$ cells/well and $20 \times 10^3$ cells/well, respectively and used for assay approximately 3 h later. $rNa_v1.8$-F-11 cells were plated at an optimized concentration of $22 \times 10^3$ cells/well and incubated overnight before assay. For electrophysiological studies cells were plated onto poly-D-lysine–coated (100 μg/ml) glass coverslips at a density that enabled isolated cells to be selected for voltage-clamp recordings and maintained under 95%/5% $O_2/CO_2$ at 37°C for 12 to 48 h before recording.

**Measurement of Membrane Potential Using the FLIPR.** Membrane potential in $rNa_v1.2a$-CHO, $hNa_v1.5$–293-EBNA, and $rNa_v1.8$-F-11 cell lines was monitored using a fluorescent membrane potential-sensitive (FMP) dye (Molecular Devices, Sunnyvale, CA) and FLIPR as described previously by Vickery et al. (2004). Membrane depolarization, or hyperpolarization, of FMP dye-loaded cells produces an increase, or decrease, respectively, in fluorescence emission.

In brief, cells were incubated with FMP dye under the conditions indicated in parentheses: $rNa_v1.2a$-CHO (50 min, 22°C), $hNa_v1.5$–293-EBNA (35 min, 22°C), and $rNa_v1.8$-F-11 (45 min, 37°C). For the final 30 min of the dye loading period, cells were incubated in the absence (i.e., control) or presence of increasing concentrations of antagonists. The plates then were placed on the FLIPR and cell fluorescence monitored ($\lambda_{ex}$, 488 nm; $\lambda_{em}$, relevant emission filter provided by Molecular Devices) before and after the addition of Hanks' balanced salt solution-HEPES buffer containing the appropriate concentrations of VGSC activators. Activation of $Na^+$ channels in $rNa_v1.2a$-CHO, $hNa_v1.5$–293-EBNA, and $rNa_v1.8$-F-11 cells was achieved using veratridine (20 μM) alone, veratridine (20 μM) plus deltamethrin (3 μM), and veratridine (20 μM) plus deltamethrin (20 μM), respectively. Fluorescence emission was monitored for 15 s before the addition of stimulus buffer to establish a baseline and then for 4 min after the addition. For $rNa_v1.8$-F-11, all additions of $Na^+$ channel activators were made at 37°C on the FLIPR. To ensure that the temperature was stable during the recording period, $rNa_v1.8$-F-11 cells were pre-equilibrated for 15 min in the FLIPR before activator addition. F-11 cells express an endogenous tetrodotoxin-sensitive VGSC; therefore, recombinant $rNa_v1.8$-F-11 cells were coincubated with 300 nM tetrodotoxin (final assay concentra-

tion after activator addition) to isolate rNa$_v$1.8-mediated depolarizations. A panel of control compounds, including tetrodotoxin, lidocaine, bupivacaine, and mexiletine, was included in all experiments to confirm the stability of VGSC expression in the respective cell lines.

Stock solutions (10 mM) of all compounds were prepared in 100% dimethyl sulfoxide, except for veratridine and deltamethrin, for which a 40 $\mu$M veratridine stock solution in 100% EtOH and 80 $\mu$M deltamethrin stock solution in 100% dimethyl sulfoxide were prepared.

**FLIPR FMP Assay Data Analysis.** FLIPR data points were taken every 2 s. For data analysis, peak fluorescence (fluorescence intensity units) was measured using the FLIPR software. Peak values were exported into Microsoft Excel and then into Prism 3.0 (GraphPad Software, San Diego, CA). Concentration-response curves were fitted to a four-parameter sigmoidal function, with a variable slope, using Prism. Data were analyzed with the assumption that a single dimer molecule bound to, and blocked, one VGSC. One-way ANOVA and post hoc Tukey's multiple comparison tests were conducted using Prism. Data represent mean ± S.D. of at least three independent experiments. All experiments were conducted at least in duplicate.

**Preparation of Neonatal Rat Dorsal Root Ganglia Primary Cultures.** Sprague-Dawley rats 1 or 2 days old were sacrificed by $CO_2$ inhalation, in accordance with the Institutional Animal Care & Use Committee regulations, and dorsal root ganglia from all spinal levels were dissected. Primary cultures of neonatal rat dorsal root ganglia cells were prepared according to a modification of the procedure described previously (Vickery et al., 2004). In brief, dorsal root ganglia were dispersed using a combination of enzymatic treatments and mechanical trituration. Dorsal root ganglia were incubated with collagenase (0.06%, 25 min at 37°C) and then trypsin (0.125%, 15 min at 37°C) before trituration with fire-polished glass Pasteur pipettes in the presence of 0.01% DNase. The final cell suspension was resuspended in Dulbecco's modified Eagle's/Ham's F12 medium containing 10% fetal bovine serum, 100 ng/ml NGF, and 10 $\mu$M arabinoside C (to suppress the growth of non-neuronal cells) and plated onto 13-mm glass coverslips coated with poly-D-lysine (10 $\mu$g/ml) and laminin (5 $\mu$g/ml) at a density that enabled isolated cells to be selected for voltage-clamp recordings. Cells were maintained at 37°C in an atmosphere of 95%/5% $O_2$/$CO_2$ for 1 to 2 days.

**Whole-Cell Voltage-Clamp.** Patch pipettes were manufactured from glass capillary tubing (borosilicate thin wall; o.d., 1.5 mm; i.d., 1.17 mm; Warner Instruments Corporation, Hamden, CT) using a P-97 Flaming-Brown pipette puller (Sutter Instrument Co., Novato, CA) and polished with a microforge (Narishige, East Meadow, NY). The measured pipette resistance was between 1 and 3 MΩ, when placed in the bath. The reference electrode consisted of an Ag/AgCl pellet placed in the external solution. The potential between the two electrodes was adjusted for zero current flow, before the establishment of a seal. rNa$_v$1.2a-CHO and hNa$_v$1.5–293-EBNA cells were superfused with an extracellular solution containing 140 mM NaCl, 4.7 mM KCl, 2.6 mM $MgCl_2$, 11 mM glucose, and 5 mM HEPES, pH 7.4 at room temperature. For recording rat dorsal root ganglia tetrodotoxin-resistant currents, the extracellular solution contained 60 mM choline, 65 mM NaCl, 5 mM $MgCl_2$, 1 mM $CaCl_2$, 5 mM KCl, 10 mM glucose, 10 mM HEPES, pH adjusted to 7.4 with NaOH, and 300 nM tetrodotoxin. For all cell types, recording pipettes were filled with an internal solution containing 120 mM CsF, 20 mM Cs-EGTA, 1 mM $CaCl_2$, 1 mM $MgCl_2$, 15 mM NaCl, and 10 mM HEPES, pH 7.2. Cells were voltage-clamped in the whole cell configuration using an Axopatch 200B amplifier (Molecular Devices). Series resistance and cell capacitance were balanced using the amplifier's internal circuitry. Access resistances were not recorded routinely. However, precautions were undertaken to minimize command voltage errors. Only cells with peak currents lower than 5 nA were used. Furthermore, the amplifier's series resistance compensation circuitry was routinely adjusted to 60 to 80% to further ensure proper voltage control. Both current and voltage waveforms were filtered at 5 kHz, digitized at 20 kHz, and stored for offline analysis. Voltage command protocols were generated by pClamp 8.0 (Axon Instruments) software driving either an Axon Digidata 1200 or 1320 digitizer.

$Na^+$ currents were elicited by depolarizing the membrane potential to either −20 or 0 mV for 10 ms, from an appropriate holding potential. Data were stored in an Axon Binary File format. The standard holding and test potentials for the different channels are indicated in parentheses: rNa$_v$1.2a (−100 mV, 0 mV), hNa$_v$1.5 (−120 mV, −20 mV), and rat dorsal root ganglia tetrodotoxin-resistant (−90 mV, 0 mV). In brief, after stabilization of the voltage clamp, $Na^+$ current magnitude was monitored, at a frequency of 0.2 Hz, for a period of 1 min. The compound was applied in the absence of any depolarizations for a 3-min. Then, in the continuous presence of compound, a 5-Hz train of 200 10-ms pulses to the appropriate test potential was applied. Peak current amplitudes for the first and 200th depolarizations were determined using pCLAMP (Axon Instruments) and then normalized to the initial current in the absence of compound. The degree of inhibition of the first and last depolarizations represents the degree of tonic and phasic block, respectively (Weiser et al., 1999).

For rat dorsal root ganglia tetrodotoxin-resistant $Na^+$ currents, in the absence of compound, there was a 23 ± 2% (mean ± S.E.M., $n$ = 6 cells) reduction in the magnitude of the final pulse in the 5-Hz train at the high stimulus frequency. To correct for this decrement in current amplitude, which occurs in the absence of drug, each normalized data value in the presence of drug was divided by that in the absence of drug.

Concentration-response curves of normalized current amplitude against compound concentrations were constructed ($n$ = 3 or more cells for each point), and the data were fitted to a four-parameter sigmoidal function using Origin (OriginLab Corp., Northampton, MA). The upper and lower asymptotes were constrained to 1 and 0, respectively.

Compound dissociation rates from hNa$_v$1.5 and rNa$_v$1.2a VGSCs were determined. After stabilization of the voltage clamp, $Na^+$ current magnitude was monitored, at a frequency of 0.2 Hz, for a period of 1 min. hNa$_v$1.5–293-EBNA or rNa$_v$1.2a-CHO cells then were exposed to the specified concentration of lidocaine or dimer according to the protocols described above. At the end of the 5-Hz stimulus train, the compound was washed out by continuous perfusion with extracellular buffer and current magnitude monitored at a frequency of 0.2 Hz for an additional 10 min. Current amplitudes were normalized to the initial current in the absence of compound and plots of normalized current amplitude against time constructed ($n$ = 3 or more cells for each point). Data (from time of compound washout) were fitted to a single exponential decay function using Origin software.

Unpaired $t$ test or one-way ANOVA and post hoc Dunnett's test were conducted using GraphPad Prism. Data represent mean ± S.D. for at least three cells.

**Materials.** Cell culture media and supplements were obtained from Invitrogen (Carlsbad, CA). The following materials were obtained from the sources indicated in parentheses: fetal bovine serum (Hyclone, Logan, UT) and FMP (Molecular Devices). All other reagents were obtained from Sigma-Aldrich (St. Louis, MO).

The following drugs were obtained from the commercial sources indicated in parentheses: deltamethrin (RU29974; Dr. Ehrenstorfer GmbH, Augsburg, Germany); veratridine, tetrodotoxin (Sigma-Aldrich); mexiletine, pimozide, bupivacaine, 4030W92, lamotrigine, compound **1** [lidocaine; 2-diethylamino-*N*-(2,6-dimethyl-phenyl)-acetamide], compound **2** [*N*-(2,6-dimethyl-phenyl)-2-[(2-{[(2,6-dimethyl-phenylcarbamoyl)-methyl]-methyl-amino}-ethyl)-methyl-amino]-acetamide], compound **3** [*N*-(2,6-dimethyl-phenyl)-2-[(3-{[(2,6-dimethyl-phenylcarbamoyl)-methyl]-methyl-amino}-propyl)-methyl-amino]-acetamide], compound **4** [THRX-170148; *N*-(2,6-dimethyl-phenyl)-2-[(4-{[(2,6-dimethyl-phenylcarbamoyl)-methyl]-methyl-amino}-butyl)-methyl-amino]-acetamide], compound **5** [*N*-(2,6-

dimethyl-phenyl)-2-[(5-{[(2,6-dimethyl-phenylcarbamoyl)-methyl]-methyl-amino}-pentyl)-methyl-amino]-acetamide], compound **6** [*N*-(2,6-dimethyl-phenyl)-2-[(6-{[(2,6-dimethyl-phenylcarbamoyl)-methyl]-methyl-amino}-hexyl)-methyl-amino]-acetamide], compound **7** [*N*-(2,6-dimethyl-phenyl)-2-[methyl-(4-methylamino-butyl)-amino]-acetamide], compound **8** [*N*-(2,6-dimethyl-phenyl)-2-{methyl-[4-(methyl-methylcarbamoylmethyl-amino)-butyl]-amino}-acetamide], and compound **9** [*N*-(4-{[(2,6-dimethyl-phenylcarbamoyl)-methyl]-methyl-amino}-butyl)-*N*-methyl-3-phenyl-propionamide] were prepared by the Theravance Inc. Medicinal Chemistry Department for Theravance Inc. research purposes only.

## Results

**Inhibition of $Na^+$ Channel Activator-Evoked Depolarization of $rNa_v1.2a$-CHO, $hNa_v1.5$–293-EBNA, and $rNa_v1.8$-F11 Cells by Lidocaine Dimers Is Dependent upon the Length of the Tether.** The interaction of the dimers with specific VGSC subtypes initially was examined using $rNa_v1.2a$-CHO, $hNa_v1.5$–293-EBNA, and $rNa_v1.8$-F-11 recombinant cell lines and a novel FLIPR membrane potential sensitive dye assay (Vickery et al., 2004). Tetrodotoxin produced a concentration-dependent inhibition of $Na^+$ channel activator-evoked depolarization of $rNa_v1.2a$-CHO, $hNa_v1.5$–293-EBNA, and $rNa_v1.8$-F-11 cells with $pIC_{50}$ values as expected for inhibition of $Na_v1.2a$, $Na_v1.5$, and $Na_v1.8$ $Na^+$ channels, respectively (Table 1). Lidocaine, and the dimers, also produced a concentration-dependent inhibition of activator-evoked depolarization in each cell type (Table 1). The potencies of the dimers were dependent upon the length of the linker and ranged from 10 to ≥100-fold higher than that of lidocaine ($p < 0.001$; Tukey's test) (Fig. 2). The rank order of potencies was similar at $rNa_v1.2a$ (compound **4** > compound **3** > compound **6** = compound **5** = compound **2** ≫ lidocaine), $hNa_v1.5$ (compound **4** > compound **3** = compound **6** = compound **5** = compound **2** ≫ lidocaine), and $rNa_v1.8$ (compound **4** > compound **3** > compound **6** = compound **5** = compound **2** ≫ lidocaine) VGSC subtypes. There were statistically significant differences between the potencies of each dimer for the three respective VGSC subtypes (one-way ANOVA, $p < 0.05$); however, these were small (≤10-fold). Thus, lidocaine and compound **2** were significantly less potent at $rNa_v1.2a$ than at both $hNa_v1.5$ and $rNa_v1.8$ subtypes, whereas compounds **5** and **6** were significantly less potent at $rNa_v1.2a$ than at $hNa_v1.5$ ($p < 0.05$, Tukey's test). Compounds **3** and **4** were significantly less potent at both $rNa_v1.2a$ and $hNa_v1.5$ subtypes than $rNa_v1.8$ ($p < 0.05$, Tukey's test). Under the present experimental conditions, the values for the Hill coefficients for the lidocaine dimers were, in general, greater than 1.0 at all VGSC subtypes. However, there were no consistent differences between the Hill slopes for the dimers and lidocaine.

To probe the specificity of the interaction of the most potent dimer, compound **4**, with VGSCs, the effects of three control compounds (compounds **7**, **8**, and **9**) (Fig. 1) were examined. These compounds make up a single lidocaine moiety coupled to a $C_4$ linker where the second lidocaine moiety has been replaced by one of three functional groups, corresponding to critical components of the local anesthetic pharmacophore, specifically an amine (positively-charged nitrogen), an amide, and an arene group (Rang and Dale, 1991). Compound **7** had no effect on $Na^+$ channel activator-evoked depolarization up to a concentration of 100 μM, the highest concentration tested (Table 1). In contrast, compounds **8** and **9** both inhibited activator-evoked depolarization, but were at least 1 order of magnitude less potent than compound **4** itself at the respective VGSC subtypes ($p <$ 0.001, Tukey's test) (Table 1).

**Lidocaine Dimers Are Potent, Strongly Use-Dependent Inhibitors of $rNa_v1.2a$, $hNa_v1.5$, and Rat Dorsal Root Ganglia Tetrodotoxin-Resistant VGSCs.** The in-

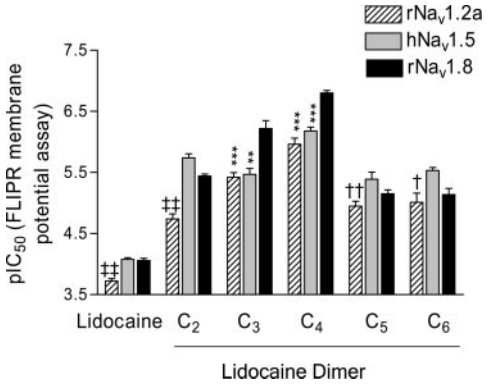


**Fig. 2.** Effect of lidocaine and compounds **2** to **6** on $Na^+$ channel activator-evoked depolarization of $rNa_v1.2a$-CHO (▨), $hNa_v1.5$–293-EBNA (▤), and $rNa_v1.8$-F-11 (■) cells. FMP dye-loaded cells were incubated for 30 min in the absence or presence of antagonist. Membrane potential in $rNa_v1.2a$, $hNa_v1.5$, and $rNa_v1.8$ cells then was monitored using a FLIPR before and after the addition of veratridine (20 μM), veratridine (20 μM) plus deltamethrin (3 μM), or veratridine (20 μM) plus deltamethrin (20 μM), respectively, to elicit membrane depolarization. Data represents mean ± S.D. of 4 to 26 independent $pIC_{50}$ determinations, each performed in duplicate. ***, $p < 0.001$, **, $p < 0.01$, significantly different from $rNa_v1.8$; ††, $p < 0.01$, †, $p < 0.05$, significantly different from $hNa_v1.5$; and ‡‡, $p < 0.01$, significantly different from both $hNa_v1.5$ and $rNa_v1.8$ (Tukey's multiple comparison test).

TABLE 1

$pIC_{50}$ values for lidocaine and lidocaine dimers at $rNa_v1.2a$, $hNa_v1.5$, and $rNa_v1.8$ recombinant VGSCs determined using FLIPR membrane potential assay

Data represents mean ± S.D. of number of observations (*n*) indicated. Activation of $Na^+$ channels in FMP-dye loaded $rNa_v1.2a$-CHO, $hNa_v1.5$–293-EBNA, and $rNa_v1.8$-F-11 cells was achieved using veratridine (20 μM), veratridine (20 μM) plus deltamethrin (3 μM), and veratridine (20 μM) plus deltamethrin (20 μM), respectively.

| | $rNa_v1.2a$ $pIC_{50}$ | *n* | $hNa_v1.5$ $pIC_{50}$ | *n* | $rNa_v1.8$ $pIC_{50}$ | *n* |
|---|---|---|---|---|---|---|
| Lidocaine | 3.7 ± 0.2 | 21 | 4.1 ± 0.1 | 26 | 4.1 ± 0.2 | 23 |
| Compound **2** | 4.7 ± 0.2 | 7 | 5.7 ± 0.1 | 4 | 5.4 ± 0.1 | 4 |
| Compound **3** | 5.4 ± 0.2 | 8 | 5.5 ± 0.2 | 4 | 6.2 ± 0.3 | 4 |
| Compound **4** | 6.0 ± 0.4 | 15 | 6.2 ± 0.2 | 11 | 6.8 ± 0.1 | 9 |
| Compound **5** | 5.0 ± 0.2 | 9 | 5.4 ± 0.3 | 6 | 5.2 ± 0.1 | 4 |
| Compound **6** | 5.0 ± 0.3 | 5 | 5.5 ± 0.1 | 4 | 5.1 ± 0.2 | 4 |
| Compound **7** | <4 | 4 | <4 | 4 | 3.5 ± 0.2 | 4 |
| Compound **8** | <4 | 4 | 4.7 ± 0.4 | 4 | 4.7 ± 0.1 | 4 |
| Compound **9** | 5.0 ± 0.2 | 4 | 4.9 ± 0.2 | 4 | 5.3 ± 0.1 | 4 |
| Tetrodotoxin | 8.7 ± 0.2 | 4 | 5.6 ± 0.2 | 22 | < 4.0 | 8 |

hibitory properties of the dimers at $rNa_v1.2a$, $hNa_v1.5$, and rat DRG tetrodotoxin-resistant VGSCs were examined using whole cell voltage-clamp techniques.

The characteristics of $hNa_v1.5$ $Na^+$ current block by lidocaine (300 $\mu$M) and the most potent dimer, compound **4** (3 $\mu$M) are illustrated by the representative raw current traces in Fig. 3, a and c, insets. Lidocaine (300 $\mu$M) inhibited the first and last pulses in the 5-Hz train by 53 ± 0.3% (tonic inhibition) and 84 ± 0.9% (phasic inhibition) ($n$ = 3 cells), respectively. In contrast, for compound **4** (3 $\mu$M), there was minimal (15 ± 8%) tonic inhibition but 80 ± 5% inhibition of the last pulse of the train (phasic inhibition) ($n$ = 3 cells). Concentration-response curves for tonic and phasic block of $hNa_v1.5$ $Na^+$ currents by lidocaine (10–300 $\mu$M) and compound **4** (0.1–30 $\mu$M) were constructed (Fig. 3, b and d), and the corresponding $pIC_{50}$ values were calculated (Table 2). Using the present voltage clamp protocols, compound **4** was approximately 60-fold more potent than lidocaine and was strongly use-dependent, with a 30-fold shift in the potency for phasic block, relative to tonic. It is noteworthy that the use-dependent component of block reached steady state rapidly for each concentration of lidocaine tested, but for compound **4**, true steady-state inhibition was not reached during the 200-pulse train (Fig. 3, a and c). This probably reflects the differences in the dissociation rates of the compounds (see below).

The characteristics of inhibition of neonatal rat tetrodotoxin-resistant $Na^+$ currents (Fig. 4), by lidocaine and compound **4**, were very similar to those for inhibition of $hNa_v1.5$ $Na^+$ currents. Compound **4** exhibited strong use-dependent inhibition of rat tetrodotoxin-resistant $Na^+$ currents. At a concentration of 3 $\mu$M, there was minimal (~ 5%) tonic inhibition but 84 ± 4% inhibition of the last pulse of the train (phasic inhibition) ($n$ = 3 cells) (Fig. 4, a and c, inset). The tonic and phasic $pIC_{50}$ values for inhibition of rat tetrodotoxin-resistant $Na^+$ currents by lidocaine and compound **4** were 3.8 and <4.5 (tonic) and 4.1 and 6.3 (phasic), respectively ($n \geq 3$ cells). Similar data were obtained for inhibition of $rNa_v1.2a$ $Na^+$ currents by lidocaine and compound **4** [$pIC_{50}$ values = < 3.5 and <4.5 (tonic) and <3.5 and 6.0 (phasic), respectively ($n \geq 3$ cells)].

In summary, under the present recording conditions, there was a small (≤10-fold) difference between the tonic potencies of lidocaine and compound **4**, compared with a 60- to 300-fold difference between the phasic potencies, at the three respective VGSC subtypes. Compound **4** was strongly use-dependent with a >30-fold difference between the tonic and phasic $IC_{50}$ values, compared with a <5-fold difference for lidocaine.

TABLE 2

Tonic and phasic inhibition of $hNa_v1.5$ $Na^+$ currents by lidocaine and lidocaine dimers determined using whole-cell voltage-clamp

Data represents mean of three cells.

| | $hNa_v1.5$ $pIC_{50}$ | |
|---|---|---|
| | Tonic | Phasic |
| Lidocaine | 3.5 | 4.2 |
| Compound **2** | 3.9 | 4.9 |
| Compound **3** | 4.2 | 5.4 |
| Compound **4** | 4.5 | 6.0 |
| Compound **5** | 4.6 | 5.8 |
| Compound **6** | 4.9 | 5.8 |
| Compound **7** | —[a] | —[a] |
| Compound **8** | 3.9 | 4.9 |
| Compound **9** | 3.8 | 5.1 |

[a] Compound disrupted gigaseal at 10 $\mu$M.

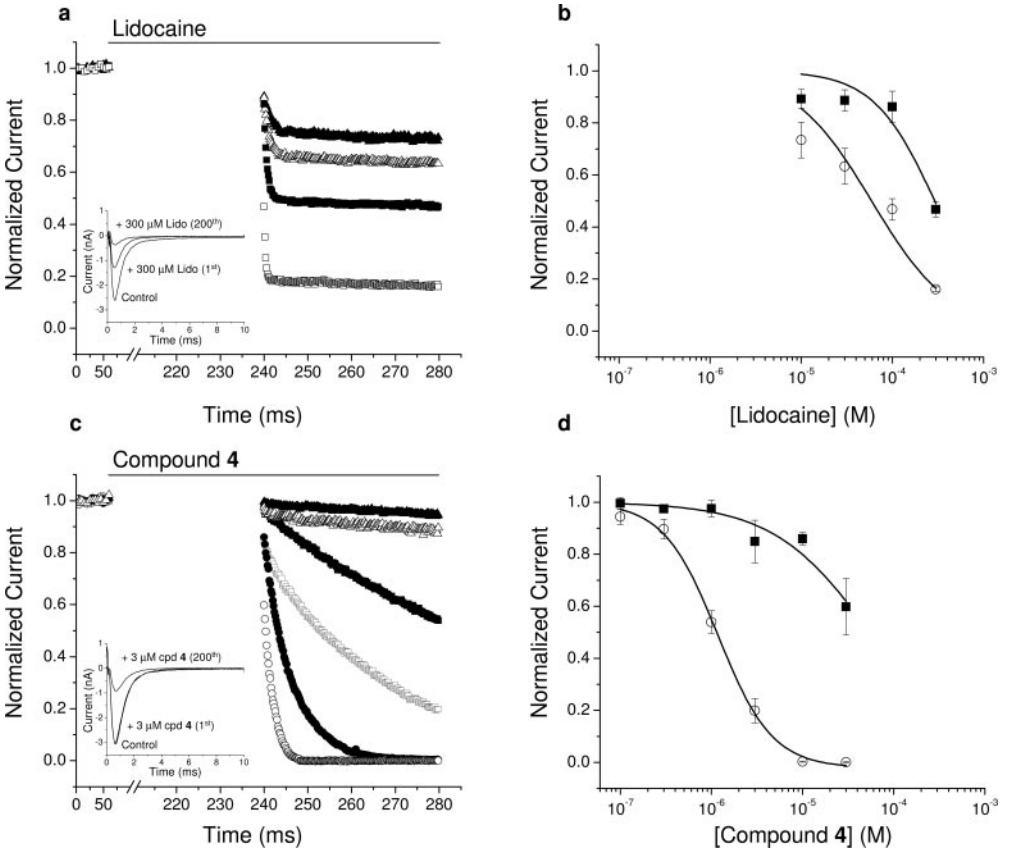


**Fig. 3.** Tonic and phasic inhibition of $hNa_v1.5$ $Na^+$ currents by lidocaine and compound **4**. Normalized current responses in the presence of increasing concentrations of lidocaine (▲, 10 $\mu$M; △, 30 $\mu$M; ■, 100 $\mu$M; □, 300 $\mu$M) (a) and compound **4** (▲, 0.1 $\mu$M; △, 0.3 $\mu$M; ■, 1 $\mu$M; □, 3 $\mu$M; ●, 10 $\mu$M; ○, 30 $\mu$M) (c). $Na^+$ current magnitude was monitored at a frequency of 0.2 Hz for 1 min. Cells were then exposed to lidocaine or compound **4** in the absence of depolarizing pulses for 3 min, followed by a 5-Hz train of 200 10-ms pulses from the holding potential (−120 mV) to the test potential (−20 mV), in the continuous presence of compound. Current amplitudes were normalized to the initial current in the absence of compound. Inset, representative current traces evoked by a single pulse in the absence of compound (control) and by pulses 1 and 200 of the train, in the presence of 300 $\mu$M lidocaine (a) or 3 $\mu$M compound **4** (cpd **4**; c). Concentration-response curves showing effect of lidocaine (b) and compound **4** (d) on the amplitude of the first (■) and last (□) depolarizations in the 200-pulse train. Data represents mean ± S.E.M. of at least three cells. In a and c, the standard error bars have been omitted for clarity.

The rank order of potency of compound **4**, for phasic inhibition of VGSC $Na^+$ currents, was rat dorsal root ganglia tetrodotoxin-resistant > $rNa_v1.2a$ = $hNa_v1.5$. However, the absolute difference in potency for inhibition of the three VGSC subtypes was ≤2-fold.

The tonic and phasic $pIC_{50}$ values for compounds **1** to **9** were determined on $hNa_v1.5$ $Na^+$ currents (Table 2). There was a reasonable correlation ($r^2 = 0.6$, slope = 0.7, $n = 8$) between the phasic and FLIPR $pIC_{50}$ values for these compounds, supporting the conclusion that the potency of the dimers is dependent upon the length of the tether. Furthermore, the dimers each exhibited use-dependent block with a difference between the tonic and phasic $IC_{50}$ values of approximately 10-fold, or greater. The control compounds, **8** and **9,** were both approximately 1 order of magnitude less potent than compound **4** for phasic block (Table 2). The kinetics of inhibition of $hNa_v1.5$ $Na^+$ currents by compound **9** were similar to those of lidocaine such that inhibition of the current reached steady-state during the 200-pulse train (data not shown). In contrast, compound **8** had a profile similar to that of compound **4**, and steady-state inhibition was not achieved during the 200-pulse train (data not shown). As noted previously, this probably reflects the differences in dissociation rates of the compounds. Unfortunately, it was not possible to assess the potency of compound **7** using voltage-clamp techniques, because at concentrations >10 μM, the compound disrupted the established giga-seal.

**The Rate of Dissociation of Lidocaine Dimers from VGSCs Is Dependent upon the Length of the Tether.** $hNa_v1.5$–293-EBNA cells were exposed to equieffective (approximately phasic $IC_{80}$) concentrations (in parentheses) of lidocaine (300 μM), compound **2** (30 μM), compound **3** (10 μM), compound **4** (3 μM), compound **5** (10 μM), compound **6** (10 μM), compound **8** (30 μM) or compound **9** (30 μM), and the rates of recovery from inhibition were determined as described under *Materials and Methods*. The effect of lidocaine was rapidly ($\tau$ < 10 s) reversible upon washout (Fig. 5a). In contrast, the dimers exhibited slower, linker length-dependent dissociation rates with $\tau$ values of 133 s, 3000 s, 41 s, and 50 s for compounds **2**, **3**, **5**, and **6**, respectively (Fig. 5a). There was negligible recovery of the $hNa_v1.5$ $Na^+$ current from inhibition by compound **4** up to 10 min after washout (Fig. 5a). It was not possible to investigate longer washout periods because of instability in the recordings at later time points, and a $\tau$ value was not determined. Therefore, the rank order for dissociation from $hNa_v1.5$ VGSCs was lidocaine > compound **5** = compound **6** > compound **2** ≫ compound **3** > compound **4**. The dissociation of compound **4** was not enhanced by changing the holding potential to a more negative potential (−140 mV), during the washout period (data not shown). In contrast to compound **4**, dissociation of both the controls, compounds **8** and **9,** could be observed. Thus, compound **9** had a rapid dissociation rate ($\tau$ < 10 s) similar to that of lidocaine, whereas compound **8** had a comparatively slower dissociation rate with a $\tau$ value of 233 s. $rNa_v1.2a$-CHO cells also were exposed to equieffective (approximate phasic $IC_{80}$) concentrations (in parentheses) of compound **2** (300 μM), compound **3** (3 μM), compound **4** (3 μM), compound **5** (30 μM), or compound **6** (10 μM), and the rates of recovery were determined. For each compound the dissociation rate from $rNa_v1.2a$ was faster than the corresponding rate from $hNa_v1.5$; however, the rank order was similar (Fig. 5b). Thus, the dissociation rates for compounds **2**, **5**, and **6** were very rapid ($\tau$ values of <10 s) whereas for

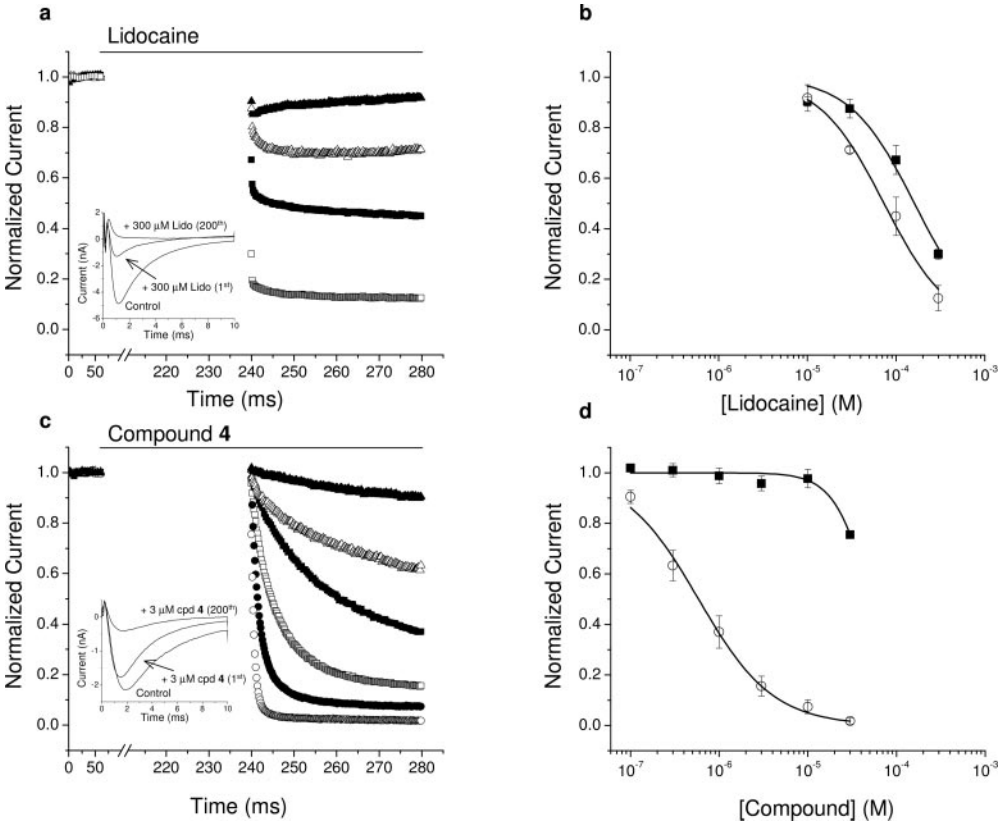


**Fig. 4.** Tonic and phasic inhibition of rat tetrodotoxin-resistant $Na^+$ currents by lidocaine and compound **4**. Normalized current responses in the presence of increasing concentrations of lidocaine (▲, 10 μM; △, 30 μM; ■, 100 μM; □, 300 μM) (a) and compound **4** (▲, 0.1 μM; △, 0.3 μM; ■, 1 μM; □, 3 μM; ●, 10 μM; ○, 30 μM) (c). $Na^+$ current magnitude was monitored at a frequency of 0.2 Hz for 1 min. Cells then were exposed to lidocaine or compound **4** in the absence of depolarizing pulses for 3 min, followed by a 5-Hz train of 200 10-ms pulses from the holding potential (−90 mV) to the test potential (−0 mV), in the continuous presence of compound. Current amplitudes were normalized to the initial current in the absence of compound and then corrected for current run down, as described under *Materials and Methods*. Inset, representative current traces evoked by a single pulse in the absence of compound (control) and by pulses 1 and 200 of the train, in the presence of 300 μM lidocaine (a) or 3 μM compound **4** (cpd **4**; c). Concentration-response curves showing effect of lidocaine (b) and compound **4** (d) on the amplitude of the first (■) and last (□) depolarizations in the 200-pulse train. Data represents mean ± S.E.M. of at least three cells. In a and c, the standard error bars have been omitted for clarity.

compounds **3** and **4** the rates were slower with $\tau$ values of 197 s and 335 s, respectively.

**Monomeric VGSC Inhibitors Attenuate Compound 4-Mediated Inhibition of hNa$_v$1.5 VGSCs.** To investigate the relationship between the well characterized local anesthetic binding site and the compound **4** binding site(s) on VGSCs, we investigated the effect of coincubation with local anesthetic receptor site inhibitors, or tetrodotoxin, on compound **4**-mediated inhibition of hNa$_v$1.5 $Na^+$ currents. hNa$_v$1.5–293-EBNA cells were incubated with compound **4** in the absence or presence of a local anesthetic or tetrodotoxin, as described under *Materials and Methods*. At the end of the stimulus train, the compounds were washed out, and current magnitude was monitored at a frequency of 0.2 Hz for a further 10 min.

Compound **4** (1 $\mu$M) produced 44 ± 7% ($n$ = 3 cells) inhibition of hNa$_v$1.5 $Na^+$ currents, which was maintained up to 10 min after washout (Fig. 6a, control), consistent with those data described in the previous section. In contrast, after coincubation with mexiletine (1 mM), but not tetrodotoxin (100 $\mu$M), negligible compound **4**-mediated inhibition was apparent after washout (Fig. 6a). Application of mexiletine (1 mM) alone or tetrodotoxin (100 $\mu$M) alone produced complete inhibition of hNa$_v$1.5 $Na^+$ currents, which recovered to predrug amplitudes within 10 s of inhibitor washout ($n$ = 3 cells, data not shown). In subsequent experiments, hNa$_v$1.5–293-EBNA cells were incubated with increasing concentrations of compound **4**, in the absence or presence of a fixed concentration of mexiletine and concentration-response curves of normalized current amplitude (at 10 min after compound washout) constructed. Coincubation with mexiletine (0.3 or 1 mM) produced parallel, rightward shifts in the compound **4** concentration-response curve (Fig. 6b). The corresponding Hill coefficients for compound **4** were 1.2, 1.1, and 1.3 in the absence and presence of 0.3 and 1 mM mexiletine, respectively. Similar experiments were conducted using lidocaine (1 mM), bupivacaine (1 mM), and pimozide (0.01 mM) (data not shown). The respective $pIC_{50}$ values for phasic inhibition were calculated and then, using the Schild equation (Arunlakshana and Schild, 1959), the apparent $pK_b$ values for the different VGSC inhibitors were determined (Table 3). There was a good correspondence between the $pK_b$ values and the respective phasic $pIC_{50}$ values at hNa$_v$1.5 (Table 2).

**Monomeric VGSC Inhibitors Increase the Rate of Dissociation of Compound 4 from hNa$_v$1.5 VGSCs.** The observation that coincubation with local anesthetic receptor site inhibitors attenuated interaction of compound **4** with hNa$_v$1.5 VGSCs is consistent with competitive antagonism.

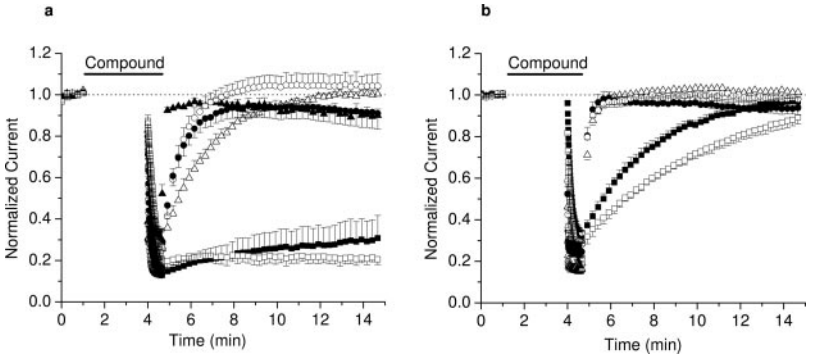


**Fig. 5.** Dissociation of lidocaine and lidocaine dimers from hNa$_v$1.5 and rNa$_v$1.2a VGSCs. hNa$_v$1.5–293-EBNA cells (a) and rNa$_v$1.2a-CHO cells (b) were exposed to lidocaine or dimer in the absence of depolarizing pulses for 3 min, followed by a 5-Hz train of 200 10-ms pulses, in the continuous presence of the compound. At the end of the train, the compound was washed out and current magnitude was monitored at a frequency of 0.2 Hz for 10 min, as described under *Materials and Methods*. Compounds were applied for the period indicated by the black bar. hNa$_v$1.5–293-EBNA cells were exposed to approximate phasic $IC_{80}$ concentrations: lidocaine (▲, 300 $\mu$M), compound **2** (△, 30 $\mu$M), compound **3** (■, 10 $\mu$M), compound **4** (□, 3 $\mu$M), compound **5** (●, 10 $\mu$M), or compound **6** (○, 10 $\mu$M) dimer. rNa$_v$1.2a-CHO cells were exposed to concentrations that corresponded to the approximate phasic $IC_{80}$ values for inhibition of hNa$_v$1.5 $Na^+$ currents: compound **2** (△, 300 $\mu$M), compound **3** (■, 3 $\mu$M), compound **4** (□, 3 $\mu$M), compound **5** (●, 30 $\mu$M), or compound **6** (○, 10 $\mu$M) dimer. Current amplitudes were normalized to the initial current in the absence of compound. Data represents mean ± S.E.M. of at least three cells. In a and b, for the purposes of clarity, only every third data point is shown.

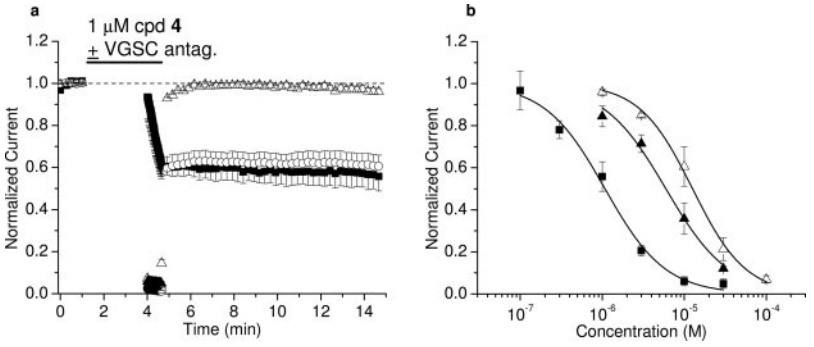


**Fig. 6.** Effect of mexiletine or tetrodotoxin on compound **4**-mediated inhibition of hNa$_v$1.5 $Na^+$ currents. a, hNa$_v$1.5–293-EBNA cells were incubated with compound **4** (1 $\mu$M) in the absence (control, ■) or presence of mexiletine (△, 1 mM) or tetrodotoxin (○, 100 $\mu$M), according to the protocol described under *Materials and Methods*. At the end of the stimulus train, the compounds were washed out, and current magnitude was monitored at a frequency of 0.2 Hz for a further 10 min. Compounds were applied for the period indicated by the black bar. b, concentration-response curves showing effect of compound **4** in the absence (■) or presence of mexiletine (▲, 300 $\mu$M; △, 1 mM) on the amplitude of the last depolarization (i.e., 10 min after drug washout). Data represents mean ± S.E.M. of at least three cells.

However, a strong negative allosteric interaction between local anesthetic receptor site inhibitors and compound **4** cannot be ruled out. To examine further the relationship between the compound **4** binding-site(s) and the local anesthetic binding site, the influence of free VGSC inhibitors on the dissociation of compound **4** from $hNa_v1.5$ VGSCs was studied.

$hNa_v1.5$–293-EBNA cells were incubated with compound **4** (10 $\mu$M), as described under *Materials and Methods*, to elicit maximal occupancy of the $hNa_v1.5$ VGSCs. At the end of the stimulus train, compound **4** was washed out and replaced with a monomeric VGSC inhibitor for a specified time ("chase period") or with a drug-free extracellular buffer (control). Current magnitude was monitored (at a frequency of 0.2 Hz) throughout the duration of the inhibitor application and, for an additional 5-min washout period, with drug-free extracellular buffer.

Under control conditions, compound **4** (10 $\mu$M) produced 94 ± 2% ($n$ = 3 cells) inhibition of $hNa_v1.5$ $Na^+$ currents, which was maintained up to 10 min after washout of the compound (Figs. 7, a and c, control). However, after chase (5 min) with increasing concentrations of lidocaine, there was a significant increase in the magnitude of the residual $Na^+$ current, determined 5 min after washout of lidocaine (Fig. 7a) (one-way ANOVA, $p < 0.0001$; Dunnett's $t$ test, $p > 0.05$, $p < 0.05$, $p < 0.01$, $p < 0.01$ for 0.3, 1.0, 3.0, and 10 mM lidocaine, respectively). Similar results were obtained with increasing concentrations of mexiletine (Fig. 7c) (one-way ANOVA, $p < 0.0001$; Dunnett's $t$ test, $p > 0.05$, $p > 0.05$, $p < 0.01$, $p < 0.01$ for 0.1, 0.3, 1.0, and 3.0 mM mexiletine, respectively). Together, these data suggest that both lidocaine and mexiletine produced a concentration-dependent increase in the rate of dissociation of compound **4** from $hNa_v1.5$ VGSCs. Consistent with the hypothesis that monomeric inhibitors increased the rate of dissociation of compound **4**, a time-dependent increase in the magnitude of the residual $Na^+$ current (determined at 5 min after washout of the inhibitor) was observed after chase (1, 5, or 10 min) with a fixed concentration of lidocaine (3 mM) or mexiletine (10 mM) (Fig. 7, b and d).

Alternate local anesthetic (bupivacaine) or anticonvulsant (lamotrigine, 4030W92) VGSC inhibitors also accelerated the dissociation of compound **4**. Thus, after a 5-min chase with a 1 mM concentration of the respective inhibitors, and a subsequent 5-min washout period, at least 40% recovery of the $hNa_v1.5$ $Na^+$ currents was observed (Table 4). In contrast, the pore-blocking toxin tetrodotoxin (100 $\mu$M) had no significant effect on compound **4** dissociation ($p > 0.38$, unpaired student's $t$ test). There was a poor correlation between the tonic and phasic potency values of the inhibitors and their ability to accelerate dissociation of compound **4** (Table 4). Thus, at a concentration of 1 mM, 4030W92 promoted the

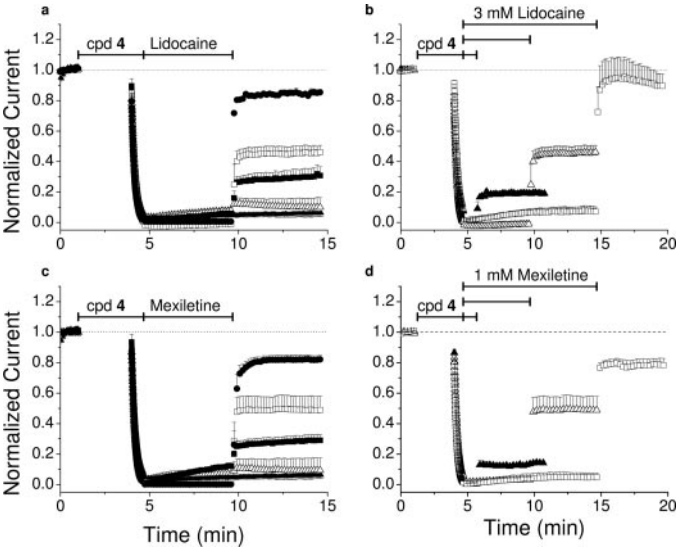


**Fig. 7.** Effect of free VGSC inhibitor on the dissociation of compound **4** from $hNa_v1.5$ VGSCs. $hNa_v1.5$–293-EBNA cells were incubated with compound **4** (10 $\mu$M) according to the standard protocol described under *Materials and Methods*, to elicit full occupancy of the $hNa_v1.5$ VGSCs. At the end of the stimulus train, compound **4** was washed out and replaced with extracellular buffer (▲, control) or inhibitor (lidocaine or mexiletine) for a specified time ("chase period"). In a and c, cells were incubated with increasing concentrations of lidocaine (△, 0.3 mM; ■, 1.0 mM; □, 3.0 mM; ●, 10 mM) (a) or mexiletine (△, 0.1 mM; ■, 0.3 mM; □, 1.0 mM; ●, 3.0 mM) (c) for a 5-min chase period. Lidocaine (3.0 mM) (c) or mexiletine (1.0 mM) (d) were applied for 1- (▲), 5- (△), or 10-min (□) chase periods. Current magnitude was monitored (at a frequency of 0.2 Hz) throughout the duration of the inhibitor application and an additional 5-min washout period, with drug-free extracellular buffer. Compounds were applied for the period(s) indicated by the black bar. Data represents mean ± S.E.M. of at least three cells.

TABLE 3

Antagonism of compound **4**-mediated inhibition of $hNa_v1.5$ $Na^+$ currents by VGSC inhibitors

Cells were coincubated with increasing concentrations of compound 4 in the absence or presence of a fixed concentration of lidocaine (1 mM), mexiletine (0.3 or 1 mM), bupivacaine (1 mM), or pimozide (10 $\mu$M), and the standard protocol (described under *Materials and Methods*) was applied. The extent of residual inhibition was determined at 10 min after washout of both compounds. Compound **4** concentration response curves (mean of $n > 3$ cells per concentration) were constructed, and $pK_b$ values for the VGSC inhibitors were determined using the Schild equation (Arunlakshana and Schild, 1959).

| VGSC Inhibitor | $hNa_v1.5$ | |
|---|---|---|
| | Apparent $pK_b$ | Phasic $pIC_{50}$ |
| Lidocaine | 4.3 | 4.2 |
| Mexiletine | | |
| 1 mM | 4.1 | 4.3 |
| 0.3 mM | 4.3 | |
| Bupivacaine | 4.8 | 5.0 |
| Pimozide | 6.4 | 5.6 |

TABLE 4

Effect of free local anesthetic, antiarrhythmic, or anticonvulsant VGSC inhibitors on the dissociation of compound **4** from $hNa_v1.5$ VGSCs

$hNa_v1.5$–293-EBNA cells were incubated with compound 4 (10 $\mu$M), as described under *Materials and Methods*, to elicit full occupancy of the $hNa_v1.5$ VGSCs. At the end of the stimulus train, compound **4** was washed out and replaced with VGSC inhibitor (at the concentrations specified), or drug-free extracellular buffer (control), for a 5-min chase period. Current magnitude was monitored (at a frequency of 0.2 Hz) throughout the duration of the inhibitor application and for an additional 5-min washout period, with drug-free extracellular buffer. The extent of recovery of the $hNa_v1.5$ $Na^+$ current, relative to the initial current amplitude, was determined at the end of the 5-min washout. Tonic and phasic $IC_{50}$ values, for the various VGSC inhibitors, were determined using the standard protocol, described in the methods ($n > 3$ cells). Recovery data represents mean ± S.E.M. ($n > 3$ cells).

| VGSC Inhibitor | $hNa_v1.5$ $IC_{50}$ | | Chase Concentration | Recovery of $Na^+$ Current |
|---|---|---|---|---|
| | Tonic | Phasic | | |
| | $\mu M$ | | $mM$ | % |
| Control | N.A. | N.A. | N.A. | 6 ± 2 |
| Lidocaine | 292 | 57 | 3 | 46 ± 5 |
| Mexiletine | 168 | 59 | 1 | 49 ± 9 |
| Bupivacaine | 94 | 12 | 1 | 53 ± 2 |
| Lamotrigine | 185 | 144 | 1 | 40 ± 3 |
| 4030W92 | >300 | 296 | 1 | 67 ± 5 |

N.A., not applicable.

greatest degree of recovery (67 ± 5%, $n = 3$) of $hNa_v1.5$ $Na^+$ currents, although this compound exhibited the lowest tonic and phasic potency values (Table 4).

Similar experiments conducted using $rNa_v1.2a$-CHO cells demonstrated that mexiletine also accelerated the dissociation of compound **4** from $rNa_v1.2a$ VGSCs. As described above, in contrast to $hNa_v1.5$, dissociation of compound **4** from $rNa_v1.2a$ could be observed in the absence of an inhibitor. Thus, under control conditions, at 10 min after washout of compound **4** (10 μM), the residual current was 77 ± 6% ($n = 3$ cells) of the initial current amplitude. In contrast, after a 5-min chase with 1 mM mexiletine, and a subsequent 5 min washout period, there was a significant increase in the residual current (112 ± 7%, $n = 3$ cells; $p = 0.02$, unpaired $t$ test).

## Discussion

The present study has demonstrated that *N*-linked lidocaine dimers, in which the lidocaine moieties are linked by an unsubstituted alkylene chain, are potent, use-dependent inhibitors of $rNa_v1.2a$, $hNa_v1.5$, and $rNa_v1.8$ VGSCs. The potency and dissociation rate of the dimers was dependent upon the length of the linker coupling the two lidocaine moieties. The *n*-butylene-linked dimer (compound **4**) was the most potent and exhibited the slowest dissociation rate.

The observation that varying the length of the linker modulated both the potency and dissociation rate of the dimers is consistent with a multivalent interaction at VGSCs (Mammen et al., 1998; Kiessling et al., 2000; Wright and Usher, 2001). A linker length-dependent increase in potency of dimeric ligands relative to the monomer has been reported for compounds interacting with cyclic nucleotide-gated (Kramer and Karpen, 1998), $SK_{Ca}$ (Galanakis et al., 1996), and nicotinic acetylcholine receptor (Rosini et al., 1999) channels. Polymer-linked cGMP dimers simultaneously occupy two binding sites on the cyclic nucleotide-gated channel. The potency and the dissociation rate of these dimers are dependent upon the length of the linker joining the two cGMP moieties, similar to the present findings. However, in contrast to cyclic nucleotide-gated channels, which are homotetramers with a cGMP binding site on each subunit, the presence of two or more distinct binding sites for local anesthetics on VGSCs has yet to be confirmed.

Additional support for a multivalent interaction comes from studies using control compounds. Thus, compound **7**, which retains the amine but lacks the amide and arene motifs of the second lidocaine moiety, had low affinity ($pIC_{50} < 4$) for VGSCs. Furthermore, compound **8**, which retains the amine and amide but lacks the arene motif, and compound **9**, which retains the arene but lacks the corresponding amine motif, although more potent VGSC inhibitors than lidocaine, were at least 10-fold less potent than compound **4** and exhibited significantly faster dissociation rates. These data suggest that the presence of a second, intact local anesthetic pharmacophore was critical to manifest the dramatic increase in potency (relative to lidocaine) and slow dissociation rate of compound **4**.

The correlation between hydrophobicity and the in vitro and in vivo efficacy of VGSC blockers is well established (Strichartz et al., 1990). In the present study, however, the most hydrophobic molecules [i.e., compounds **5** and **6** (the relative increase in logD value being ~ 0.5 per methylene unit)] had lower in vitro potencies and exhibited significantly faster dissociation rates from VGSCs than compounds **3** or **4**. Differences in local anesthetic $pK_a$ values and hence the relative proportions of cationic and uncharged free amine forms, also can influence the extent and/or kinetics of inhibition of VGSCs (Chernoff and Strichartz, 1990). The calculated $pK_a$ value (Pallas; CompuDrug International, Inc., Sedona, AZ) for lidocaine is 8.03. In comparison, for the dimers, the calculated $pK_a$ values for the amine in the first lidocaine moiety range from 6.83 (compound **2**) to 8.23 (compounds **5** and **6**) and in the second moiety from 3.79 (compound **2**) to 7.62 (compounds **5** and **6**). Therefore, it is possible that, except for compounds **5** and **6**, which are diprotonated, all the dimers exist as monoprotonated, or even uncharged (i.e., compound **2**) species at physiological pH. The observation that compound **8**, which has calculated $pK_a$ values (7.09, 6.67) very similar to those of compound **4** (7.37, 6.37), yet exhibited lower potency and a more rapid dissociation rate, is consistent with the proposal that differences in charge state alone are unlikely to account for the dramatic increase in potency and/or kinetic properties of compound **4**. To summarize, it is proposed that the specific structure of compound **4** (as discussed above), and not simply its physical properties (i.e., hydrophobicity, charge state), accounts for the slow dissociation rate and enhanced potency at VGSCs.

The strongest evidence for a bivalent interaction of a lidocaine dimer with VGSCs derives from the observation that free local anesthetics increase the dissociation of compound **4** from $hNa_v1.5$ and $rNa_v1.2a$. In monovalent binding, the dissociation of a ligand from its binding site is determined by the rate constant for dissociation and is unaffected by the concentration of a competing free ligand in solution. However, in bivalent binding, dissociation occurs in stages, and its rate can be accelerated by occupancy of either site by monovalent

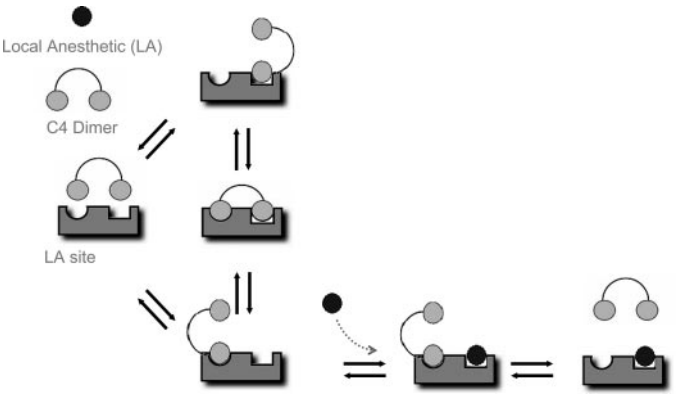


**Fig. 8.** Schematic representation of a putative model for interaction of lidocaine dimers with VGSCs. The lidocaine dimer simultaneously occupies two proximal binding sites on the VGSC, one of which is the conventional local anesthetic site (denoted "LA site", semicircular) and the second an as-yet-undefined site (rectangular). When one of the lidocaine moieties in the dimer dissociates, it has a high probability of rebinding before its partner can also dissociate. This results in a decrease in the dissociation rate of the dimer. Occupancy of the binding site with competing ligand [i.e., free local anesthetic (or alternate VGSC inhibitor)] prevents this rebinding event and hence speeds the dissociation of the dimer. For the purposes of clarity, only those interactions that are most relevant to the hypothetical model are shown. Therefore, interaction of free local anesthetic at the "LA site" is not shown, given the poor correlation between the tonic and phasic potency values of local anesthetic ligands and their ability to accelerate dissociation of the dimer.

ligand (Fig. 8; Kramer and Karpen, 1998). One interpretation of the present findings is that compound **4** binds to the conserved local anesthetic receptor and a second site. The binding of compound **4** to $hNa_v1.5$ VGSCs was inhibited, in an apparently competitive manner, by coincubation with local anesthetic, anticonvulsant, or antiarrhythmic agents, with estimated $pK_b$ values similar to their corresponding phasic $pIC_{50}$ values. These data are consistent with the hypothesis that one of the binding sites for compound **4** is the conserved local anesthetic receptor. Free monovalent local anesthetics could accelerate dissociation of compound **4** through occupancy of this site. However, the apparent lack of correlation between the ability of such ligands to enhance the dissociation rate of compound **4** and their affinities for the conserved local anesthetic site suggests instead that these monovalent ligands have some affinity for the second site, and it is through interaction at this site that they promote dissociation of compound **4** (Fig. 8).

The lidocaine dimers may span adjacent domains in the VGSC or, alternatively, bind to vicinal binding sites in the protein, as has been proposed for dequalinium binding to $SK_{Ca}$ channels (Galanakis et al., 1996). A low-resolution (19 Å) three-dimensional structure of the VGSC has revealed a pseudotetrameric arrangement of the channel (Sato et al., 2001). Furthermore, as discussed previously, various amino acid residues in transmembrane region S6 from domains 1, 3, and 4 have been shown to be important for local anesthetic binding to VGSCs. However, it is believed that this reflects a domain interface binding site in which individual amino acid residues from the different S6 regions make binding interactions with the inhibitor, rather than the presence of independent binding sites (Catterall, 2002). Nevertheless, several groups have suggested the presence of additional binding sites for local anesthetics on VGSCs. The presence of two binding sites was proposed as one explanation for the influence of $Na^+$ channel activators on stereoselective inhibition by bupivacaine and other local anesthetics (Lee-Son et al., 1992). More recently, the presence of one or more additional binding sites, which are unmasked upon channel activation, has been proposed for both lidocaine (Leuwer et al., 2004) and prenylamine (Mujtaba et al., 2001). Indeed, voltage-clamp and site-directed mutagenesis techniques suggest that prenylamine and bupivacaine act at separate pharmacological receptors on $hNa_v1.5$ (Mujtaba et al., 2002). Finally, interactions between lidocaine and structural regions of $hNa_v1.5$ (Bennett et al., 1995) or $rNa_v1.2a$ (Kuroda et al., 1996, 2000), which are responsible for inactivation, have been reported.

The present findings of a small (≤10-fold) difference between the tonic potencies of lidocaine and compound **4**, compared with the dramatic (60- to 300-fold) difference between the phasic potencies, suggests that conformational changes in VGSCs, upon depolarization, expose an additional binding site and/or binding interaction(s) for the second lidocaine moiety, and the resultant multivalent interaction underlies the enhanced phasic potency and slow dissociation rate of compound **4**.

One advantage of multivalent ligands is that, in addition to an increase in potency, such compounds may exhibit increased selectivity as a result of bridging between proximal binding sites that have alternate structure and/or spatial localization on target proteins (Wright and Usher, 2001). In the present study, although the dimers exhibited significant increases in potency relative to lidocaine, they did not exhibit significant subtype selectivity, suggesting that the identity, orientation, and/or distance between the relevant binding sites must be similar for the three VGSCs. This may not be surprising because the nine sodium channel isoforms ($Na_v1.1$-$Na_v1.9$) are more than 50% identical in amino acid sequence in the extracellular and transmembrane domains (Goldin et al., 2000). Furthermore, in the putative local anesthetic binding site in D4S6, the critical phenylalanine and tyrosine residues (Catterall, 2002) are conserved among $Na_v1.2a$, $Na_v1.5$, and $Na_v1.8$. However, there were significant differences in the rates of dissociation of the dimers from $rNa_v1.2a$ and $hNa_v1.5$ that may reflect subtle differences in the interaction with these channels.

In summary, these studies have demonstrated that *N*-linked lidocaine dimers, tethered by unsubstituted alkylene linkers of varying length, are potent, use-dependent VGSC inhibitors. Both the potency and dissociation rate of the dimers was dependent upon the length of the linker coupling the two lidocaine moieties, consistent with a multivalent interaction. Furthermore, the present data suggest that a four-carbon alkylene chain provides the optimal three-dimensional orientation for binding within the series, with both lidocaine moieties in compound **4** making specific contacts with the VGSC. The observation that monomeric VGSC inhibitors accelerate the dissociation of compound **4** supports the hypothesis that compound **4** simultaneously occupies two binding sites on VGSCs. Both sites can be bound by local anesthetic, anticonvulsant, or antiarrhythmic agents, one being the conventional local anesthetic site and the other an as-yet-undefined site.

**Acknowledgments**

We thank Mathai Mammen for helpful discussion during the preparation of the manuscript.

**References**

Arunlakshana O and Schild HO (1959) Some quantitative uses of drug antagonists. *Br J Pharmacol* **14:**48–58.
Bean BP, Cohen CJ, and Tsien RW (1983) Lidocaine block of cardiac sodium channels. *J Gen Physiol* **81:**613–642.
Bennett PB, Valenzuela C, Chen LQ, and Kallen RG (1995) On the molecular nature of the lidocaine receptor of cardiac $Na^+$ channels. Modification of block by alterations in the α-subunit-IV interdomain. *Circ Res* **77:**584–592.
Catterall WA (2000) From ionic currents to molecular mechanisms: the structure and function of voltage-gated sodium channels. *Neuron* **26:**13–25.
Catterall WA (2002) Molecular mechanisms of gating and drug block of sodium channels. *Novartis Found Symp* **241:**206–218.
Cestele S and Catterall WA (2000) Molecular mechanisms of neurotoxin action on voltage-gated sodium channels. *Biochimie* **82:**883–892.
Chernoff DM and Strichartz GR (1990) Kinetics of local anesthetic inhibition of neuronal sodium currents. pH and hydrophobicity dependence. *Biophys J* **58:**69–81.
Christopoulos A, Grant MK, Ayoubzadeh N, Kim ON, Sauerberg P, Jeppesen L, and El-Fakahany EE (2001) Synthesis and pharmacological evaluation of dimeric muscarinic acetylcholine receptor agonists. *J Pharmacol Exp Ther* **298:**1260–1268.
Galanakis D, Ganellin CR, Dunn PM, and Jenkinson DH (1996) On the concept of a bivalent pharmacophore for SKCa channel blockers: synthesis, pharmacological testing, and radioligand binding studies on mono-, bis- and tris-quinolinium compounds. *Arch Pharm (Weinheim)* **329:**524–528.
Goldin AL, Barchi RL, Caldwell JH, Hofmann F, Howe JR, Hunter JC, Kallen RG, Mandel G, Meisler MH, Netter YB, et al. (2000) Nomenclature of voltage-gated sodium channels. *Neuron* **28:**365–368.
Halazy S, Perez M, Fourrier C, Pallard I, Pauwels PJ, Palmier C, John GW, Valentin JP, Bonnafous R, and Martinez J (1996) Serotonin dimers: application of the bivalent ligand approach to the design of new potent and selective 5-HT(1B/1D) agonists. *J Med Chem* **39:**4920–4927.
Hille B (2001) The superfamily of voltage-gated ion channels, in *Ion Channels of Excitable Membranes*, pp 61–93, Sinauer Associates, Sunderland, MA.
Hockerman GH, Johnson BD, Abbott MR, Scheuer T, and Catterall WA (1997) Molecular determinants of high affinity phenylalkylamine block of L-type calcium

channels in transmembrane segment IIIS6 and the pore region of the $\alpha$1 subunit. *J Biol Chem* **272:**18759–18765.
Hondeghem LM and Katzung BG (1977) Time- and voltage-dependent interactions of antiarrhythmic drugs with cardiac sodium channels. *Biochim Biophys Acta* **472:** 373–398.
Joslyn AF, Luchowski E, and Triggle DJ (1988) Dimeric 1,4-dihydropyridines as calcium channel antagonists. *J Med Chem* **31:**1489–1492.
Kiessling LL, Strong LE, and Gestwicki JE (2000) Principles for multivalent ligand design. *Annu Rep Med Chem* **35:**321–330.
Kizuka H and Hanson RN (1987) Beta-adrenoceptor antagonist activity of bivalent ligands. 1. Diamide analogues of practolol. *J Med Chem* **30:**722–726.
Kramer RH and Karpen JW (1998) Spanning binding sites on allosteric proteins with polymer-linked ligand dimers. *Nature (Lond)* **395:**710–713.
Kuroda Y, Miyamoto K, Tanaka K, Maeda Y, Ishikawa J, Hinata R, Otaka A, Fujii N, and Nakagawa T (2000) Interactions between local anesthetics and $Na^+$ channel inactivation gate peptides in phosphatidylserine suspensions as studied by 1H-NMR spectroscopy. *Chem Pharm Bull (Tokyo)* **48:**1293–1298.
Kuroda Y, Ogawa M, Nasu H, Terashima M, Kasahara M, Kiyama Y, Wakita M, Fujiwara Y, Fujii N, and Nakagawa T (1996) Locations of local anesthetic dibucaine in model membranes and the interaction between dibucaine and a $Na^+$ channel inactivation gate peptide as studied by 2H- and 1H-NMR spectroscopies. *Biophys J* **71:**1191–1207.
LeBoulluec KL, Mattson RJ, Mahle CD, McGovern RT, Nowak HP, and Gentile AJ (1995) Bivalent indoles exhibiting serotonergic binding affinity. *Bioorg Med Chem Lett* **5:**123–126.
Lee-Son S, Wang GK, Concus A, Crill E, and Strichartz G (1992) Stereoselective inhibition of neuronal sodium channels by local anesthetics. Evidence for two sites of action? *Anesthesiology* **77:**324–335.
Leuwer M, Haeseler G, Hecker H, Bufler J, Dengler R, and Aronson JK (2004) An improved model for the binding of lidocaine and structurally related local anaesthetics to fast-inactivated voltage-operated sodium channels, showing evidence of cooperativity. *Br J Pharmacol* **141:**47–54.
Mammen M, Choi S-K, and Whitesides GM (1998) Polyvalent interactions in biological systems: implications for design and use of multivalent ligands and inhibitors. *Angew Chem Int Ed Engl* **37:**2754–2794.
Mujtaba MG, Gerner P, and Wang GK (2001) Local anesthetic properties of prenylamine. *Anesthesiology* **95:**1198–1204.
Mujtaba MG, Wang SY, and Wang GK (2002) Prenylamine block of Nav1.5 channel is mediated via a receptor distinct from that of local anesthetics. *Mol Pharmacol* **62:**415–422.
Nau C, Wang SY, Strichartz GR, and Wang GK (1999) Point Mutations at N434 in D1–S6 of Mu1 $Na^+$ channels modulate binding affinity and stereoselectivity of local anesthetic enantiomers. *Mol Pharmacol* **56:**404–413.
Portoghese PS, Nagase H, Lipkowski AW, Larson DL, and Takemori AE (1988) Binaltorphimine-related bivalent ligands and their kappa opioid receptor antagonist selectivity. *J Med Chem* **31:**836–841.
Ragsdale DS, McPhee JC, Scheuer T, and Catterall WA (1996) Common molecular determinants of local anesthetic, antiarrhythmic and anticonvulsant block of voltage-gated $Na^+$ channels. *Proc Natl Acad Sci USA* **93:**9270–9275.
Ragsdale DS, Scheuer T, and Catterall WA (1991) Frequency and voltage-dependent inhibition of type IIA $Na^+$ channels, expressed in a mammalian cell line, by local anesthetic, antiarrhythmic and anticonvulsant drugs. *Mol Pharmacol* **40:**756–765.
Rang HP and Dale M (1991) Local anesthetics and other drugs that affect excitable membranes, in *Pharmacology*, 2nd ed., pp 746–761, Churchill Livingstone, New York.
Rosini M, Budriesi R, Bixel MG, Bolognesi ML, Chiarini A, Hucho F, Krogsgaard-Larsen P, Mellor IR, Minarini A, Tumiatti V, et al. (1999) Design, synthesis and biological evaluation of symmetrically and unsymmetrically substituted methoctramine-related polyamines as muscular nicotinic receptor noncompetitive antagonists. *J Med Chem* **42:**5212–5223.
Sato C, Ueno Y, Asai K, Takahashi K, Sato M, Engel A, and Fujiyoshi Y (2001) The voltage-sensitive sodium channel is a bell-shaped molecule with several cavities. *Nature (Lond)* **409:**1047–1051.
Strichartz GR, Sanchez V, Arthur GR, Chafetz R, and Martin D (1990) Fundamental properties of local anesthetics. II. Measured octanol:buffer partition coefficients and p$K_a$ values of clinically used drugs. *Anesth Analg* **71:**158–170.
Vickery RG, Amagasu SM, Chang R, Mai N, Kaufman E, Martin J, Hembrador J, O'Keefe MD, Gee C, Marquess D, et al. (2004) Comparison of the Pharmacological properties of rat Na(v)1.8 with rat Na(v)1.2a and human Na(v)1.5 voltage-gated sodium channel subtypes using a membrane potential sensitive dye and FLIPR. *Recept Channels* **10:**11–23.
Wang SY, Nau C, and Wang GK (2000) Residues in $Na^+$ channel D3–S6 segment modulate both batrachotoxin and local anesthetic affinities. *Biophys J* **79:**1379–1387.
Weiser T, Qu Y, Catterall WA, and Scheuer T (1999) Differential interaction of *R*-mexiletine with the local anesthetic receptor site on brain and heart sodium channel $\alpha$-subunits. *Mol Pharmacol* **56:**1238–1244.
Wright D and Usher L (2001) Multivalent Binding in the Design of Bioactive Compounds. *Curr Org Chem* **5:**1107–1131.
Yarov-Yarovoy V, Brown J, Sharp EM, Clare JJ, Scheuer T, and Catterall WA (2001) Molecular determinants of voltage-dependent gating and binding of pore-blocking drugs in transmembrane segment IIIS6 of the $Na^+$ channel $\alpha$ subunit. *J Biol Chem* **276:**20–27.
Yarov-Yarovoy V, McPhee JC, Idsvoog D, Pate C, Scheuer T, and Catterall WA (2002) Role of amino acid residues in transmembrane segments IS6 and IIS6 of the $Na^+$ channel $\alpha$ subunit in voltage-dependent gating and drug block. *J Biol Chem* **277:**35393–35401.

**Address correspondence to:** Jacqueline Smith, Theravance Inc., 901 Gateway Blvd., South San Francisco, CA 94080. E-mail: jsmith@theravance.com